International Journal of Technology and Applied Science (IJTAS)
E-ISSN: 2230-9004 ● Website: www.ijtas.com ● Email: editor@ijtas.com

Aerodynamic Behavior of Optimized Panels: A Comparative Study of Lift Force Responses under Variable Wind Speeds

Dr. Panga Surendra Reddy

Lecturer in Physics
General Section, Government Polytechnic Proddatur, Andhra Pradesh, India-516360

Abstract:
The aerodynamic performance of structural panels is an important consideration in applications where wind-induced forces influence structural stability, durability, and overall performance. This study presents a comparative numerical investigation of the lift force response of conventional and optimized panel designs subjected to airflow at an angle of attack (AOA) of 0° under two different inlet velocities of 5 m/s and 25 m/s. Time-dependent lift forces were evaluated to assess the influence of panel optimization on aerodynamic loading under both normal and critical flow conditions.
The results indicate that the conventional panel experiences significantly higher lift forces than the optimized panel at both airflow velocities. At an inlet velocity of 5 m/s, the conventional panel exhibits a maximum reverse lift force of approximately 400 N, which decreases to about 220 N in the positive direction. In contrast, the optimized panel records a reduced maximum reverse lift force of approximately 250 N and a positive lift force of nearly 100 N. Under the critical airflow velocity of 25 m/s, the conventional panel develops a peak reverse lift force of approximately 6000 N before decreasing to around 700 N, whereas the optimized panel limits the maximum reverse lift force to nearly 2000 N, although noticeable fluctuations are observed throughout the simulation period.
The comparative analysis demonstrates that the optimized panel effectively reduces aerodynamic lift forces and associated loading under varying flow conditions. The substantial reduction in peak lift forces suggests improved aerodynamic stability and enhanced structural performance compared with the conventional design. These findings highlight the effectiveness of panel optimization as a viable approach for minimizing wind-induced aerodynamic loads and improving the reliability of structures exposed to different airflow environments.

Keywords: Aero Dynamics Performance Optimized Panel, Lift Force, Wind Loading.

1. Introduction

Aerodynamic performance plays a crucial role in the design and optimization of panels exposed to moving air, particularly in applications such as renewable energy systems, aerospace structures, building components, and vehicle technologies. When a panel is subjected to wind, the interaction between the airflow and its surface generates aerodynamic forces, including lift and drag. These forces are strongly influenced by factors such as panel geometry, surface configuration, angle of attack, wind speed, and flow conditions. Understanding these relationships is essential for developing panel designs that can achieve improved aerodynamic efficiency, stability, and structural performance.

The optimization of panel geometry provides an opportunity to control airflow characteristics and modify the distribution of pressure over the panel surface. Optimized panels may reduce undesirable flow separation and improve the generation or management of aerodynamic forces compared with conventional configurations. However, the aerodynamic response of an optimized panel can vary significantly as wind speed changes. Therefore, examining lift-force behavior over a range of wind speeds is important for determining the effectiveness and operating characteristics of different panel designs.

The present study focuses on the aerodynamic behavior of optimized panels by comparatively analyzing their lift-force responses under variable wind speeds. The research investigates how changes in wind velocity influence the lift generated by optimized panel configurations and compares their aerodynamic responses under similar flow conditions. Through this comparative analysis, the study aims to identify variations in lift behavior, evaluate the influence of panel optimization on aerodynamic performance, and establish a better understanding of the relationship between wind speed and lift force. The findings may contribute to the development of more efficient and aerodynamically suitable panel designs for applications where wind-induced forces are a significant design consideration.

2. Methodology

2.1 Computational Model

A computational fluid dynamics (CFD) analysis was performed using **ANSYS Fluent** to investigate the aerodynamic performance of conventional and optimized panel configurations. The objective of the study was to evaluate and compare the lift forces generated on both panels under different airflow conditions. Three-dimensional geometric models of the conventional and optimized panels were developed and imported into the ANSYS Workbench environment for numerical simulation.

2.2 Geometry and Mesh Generation

The geometries of the conventional and optimized panels were created using CAD software and imported into **ANSYS Space Claim/Design Modeler**. A computational fluid domain was generated around each panel to accurately represent the external airflow. The dimensions of the fluid enclosure were selected to minimize blockage effects and prevent boundary interference.

The computational domain was discretized using an unstructured tetrahedral mesh with localized refinement near the panel surfaces and wake region to capture boundary-layer effects and flow separation accurately. Inflation layers were generated along the panel surfaces to improve near-wall resolution and accurately predict aerodynamic forces. A mesh independence study was conducted by comparing lift force values obtained from coarse, medium, and fine meshes, and the mesh providing converged results was selected for all simulations.

2.3 Governing Equations

The airflow was assumed to be incompressible, turbulent, and Newtonian. The governing equations solved in ANSYS Fluent included:

- Continuity equation (mass conservation)
- Three-dimensional Navier–Stokes momentum equations
- Turbulence transport equations

The Reynolds-Averaged Navier–Stokes (RANS) equations were employed together with the **Shear Stress Transport (SST) k–ω turbulence model**, which provides reliable prediction of adverse pressure gradients, boundary-layer development, and flow separation around bluff bodies.

2.4 Boundary Conditions

The computational domain was assigned the following boundary conditions:

- **Inlet:** Uniform velocity inlet with airflow velocities of **5 m/s** and **25 m/s**
- **Angle of Attack (AOA): 0°**
- **Outlet:** Pressure outlet with atmospheric pressure
- **Panel Surface:** No-slip wall condition
- **Side and Top Boundaries:** Symmetry or slip-wall boundary conditions to eliminate artificial wall effects

The simulations were performed under standard atmospheric conditions with air properties defined as:

- Density: **1.225 kg/m³**
- Dynamic viscosity: **1.789×10^{-5} kg/m·s**

2.5 Solver Settings

A pressure-based transient solver was employed to capture the time-dependent variation of aerodynamic lift forces. Pressure–velocity coupling was achieved using the SIMPLE algorithm, while second-order discretization schemes were adopted for pressure, momentum, and turbulence equations to improve numerical accuracy. The transient simulations were performed using an appropriate time step to ensure numerical stability and temporal resolution of the fluctuating aerodynamic forces. Residual convergence criteria of **10^{-6}** were specified for continuity, momentum, and turbulence equations.

2.6 Aerodynamic Force Evaluation

The lift force acting on each panel was monitored throughout the transient simulation. Force monitors were defined in ANSYS Fluent to record instantaneous lift values as a function of time. The numerical results were exported and plotted to compare the aerodynamic response of the conventional and optimized panels under both normal (5 m/s) and critical (25 m/s) airflow conditions.

3. Data Analysis

The time-history plots of lift force were analyzed to evaluate the peak aerodynamic loads, force fluctuations, and overall stability of the two panel configurations. The conventional and optimized panels were compared based on maximum lift force, minimum lift force, transient response, and force reduction achieved through optimization. The numerical results demonstrate the effectiveness of the optimized panel in reducing aerodynamic loading under varying airflow velocities, thereby improving aerodynamic stability and structural performance. The below charts illustrate the time vs lift force induced on the conventional and optimized panels which are subjected to air flow with an AOA of 0o and velocities 5 m/s and 25 m/s. Plots 1 and 3 depict the lift forces induced on the conventional panels when they are subjected to normal and critical velocities. The forces induced when the panels are experiencing an air flow with a velocity of 5 m/s are a maximum of 400 N in reverse direction and they tend to decrease to approximately 220N in positive direction, whereas, the forces induced are a maximum of 6000 N and gradually decrease to around 700 N when the panels are exposed to a velocity of 25 m/s. On the other hand, the forces in optimized panels are 250 N in reverse direction and when the direction is changed there is a drastic change reaching a magnitude of 100 N in positive direction, while the forces induced in the panels are a maximum of 2000 N in reverse direction and tend to change

International Journal of Technology and Applied Science (IJTAS)

E-ISSN: 2230-9004 ● Website: www.ijtas.com ● Email: editor@ijtas.com

randomly in the time period when the panels are experiencing an air flow of 25 m/s as illustrated in plot 2 and plot 4 respectively. These plots are deciphered and the numerical representation is shown in Table 1

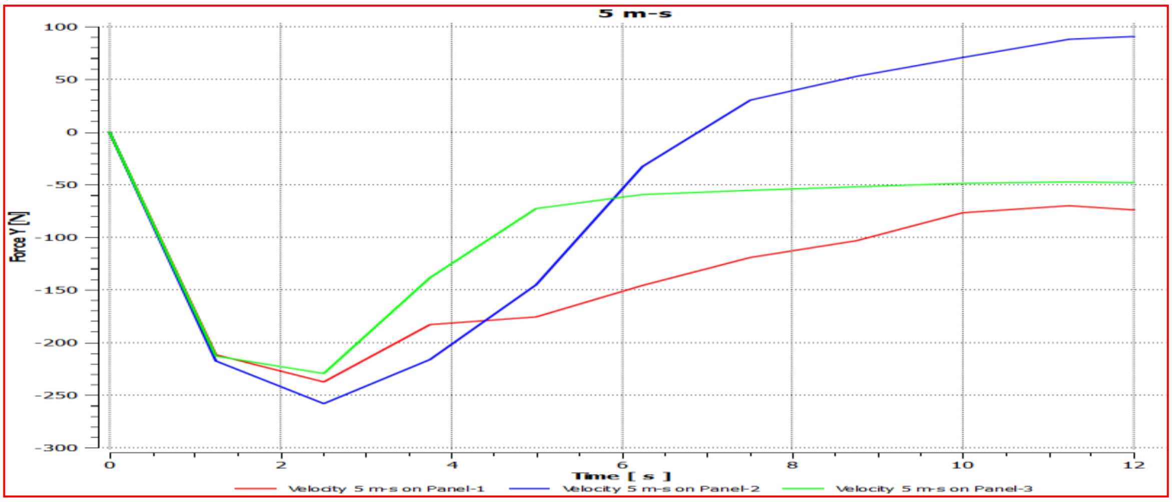

Plot.1 Time vs lift force induced on roof mounted solar panels with θ= 0°, U= 5 m/s

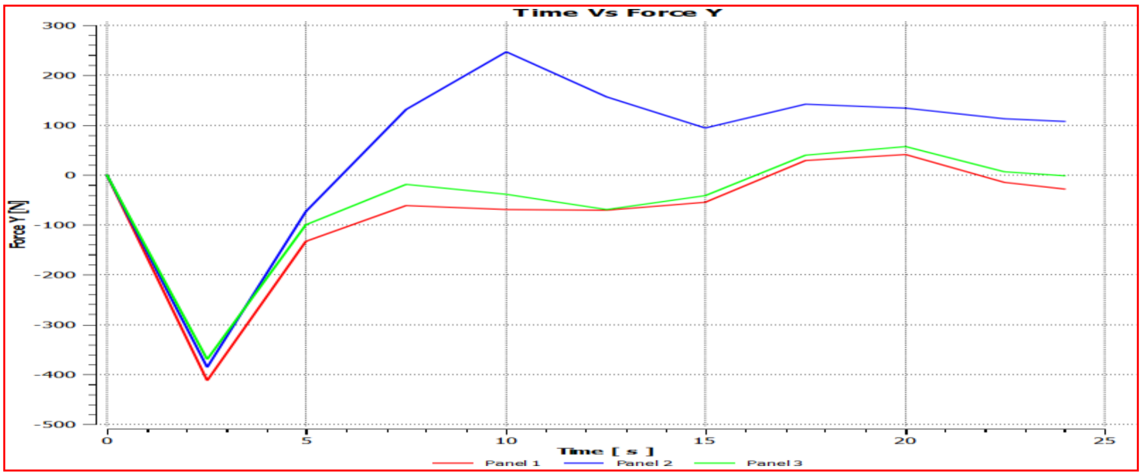

Plot.2 Time vs lift force induced on roof mounted optimized solar panels with θ= 0°, U= 5 m/s

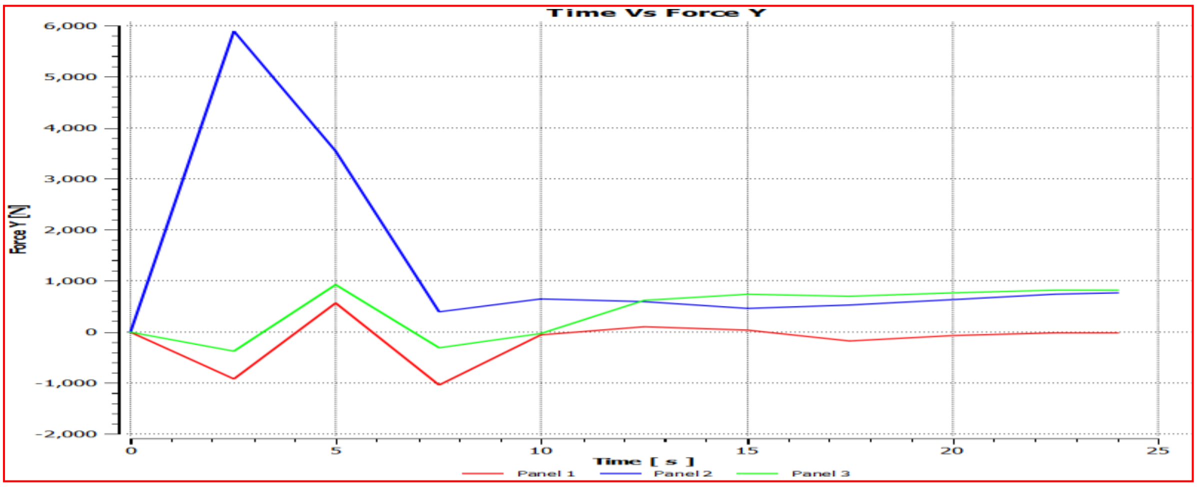

Plot.3 Time vs lift force induced on roof mounted solar panels with θ= 0°, U= 25 m/s

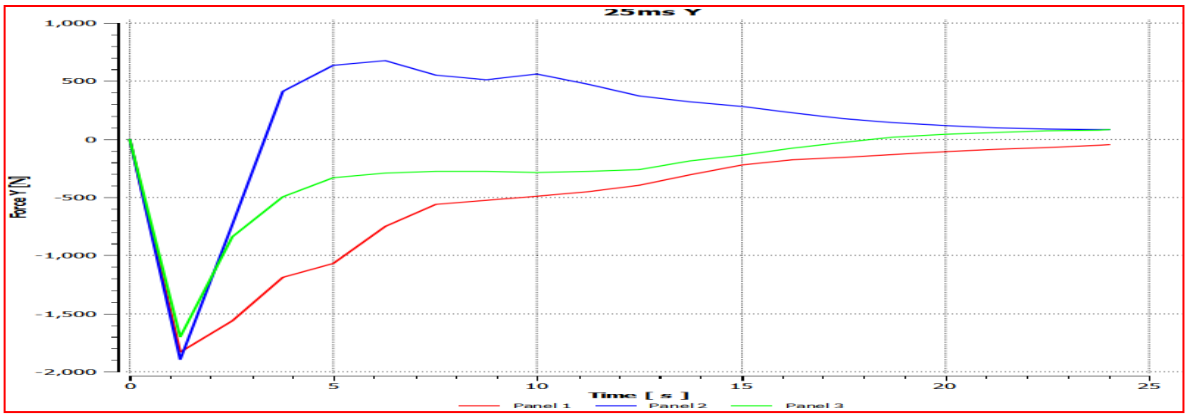

Plot.4 Time vs drag force induced on roof mounted optimized solar panels with θ= 0°, U= 25 m/s

Table.1 Lift force (Newton) comparison roof mounted solar panels at θ=0°

Panel No	5m/s Conventional	5m/s Optimized	25m/s Conventional	25m/s Optimized
Panel 1	412.576	400.16	284.19	211.943
Panel 2	385.285	393.84	322.69	196.039
Panel 3	369.217	339.76	311.77	248.29

In this test case, the panels are tested under the operating conditions of wind flow with an AOA of 45° and velocities 5 m/s and 25 m/s. The plots represent the time vs lift forces induced i.e.; the representation of the lift forces induced at different time periods. The numerical representation of these plots is presented in a tabular format in Table 2. Plots 5 and 6 hold the information of the conventional and optimized panels which are exposed to a wind flow of 5 m/s. From these plots, the maximum lift force induced on rectangular panels is 400 N in reverse direction and it finally attained the value in the range of 100 N to 200 N in positive direction during the time period, whereas the forces induced in the optimized panels are of a maximum magnitude of 150 N in reverse direction. On the other hand, when the panels are subjected to a velocity of 25 m/s, the magnitude of the forces induced is in range of 1000

N to 1000 N throughout the time period in rectangular panels and in range of 2000 N to 100 N in optimized panels. These plots are deciphered and the numerical representation is shown in Table 2.

Plot.5 Time vs lift force induced on roof mounted solar panels with θ=45°, U=5m/s

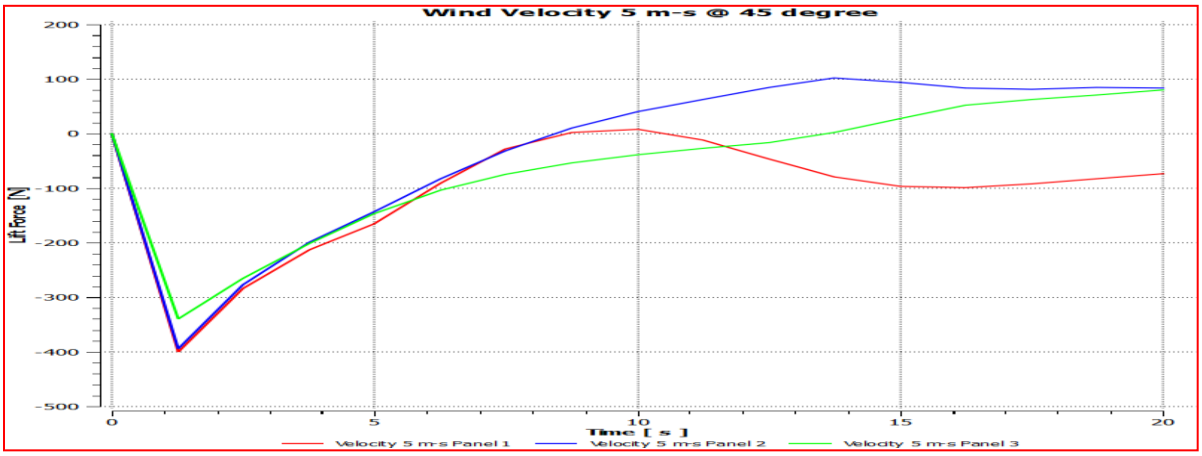

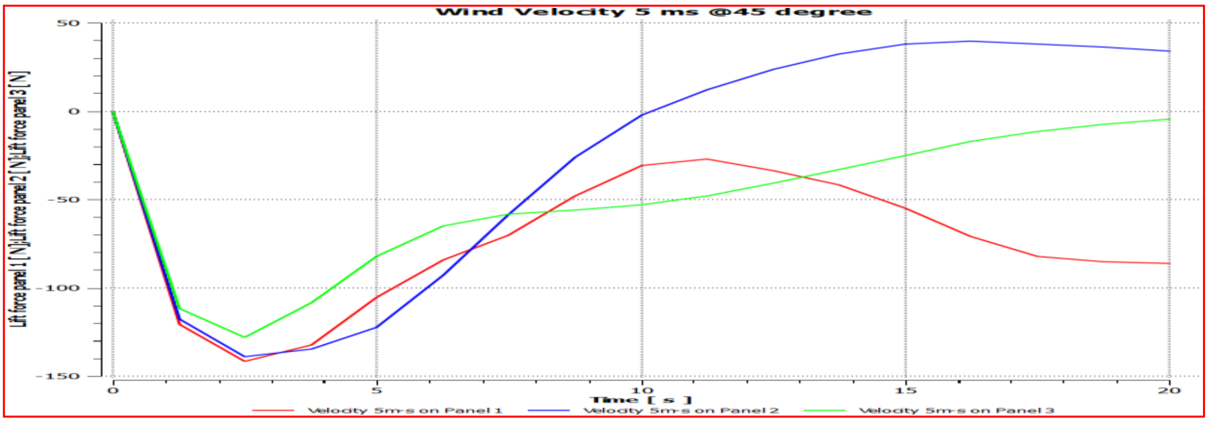

Plot.6 Time vs Lift force induced on Roof mounted Optimized panels with θ= 45°, U= 5m/s m

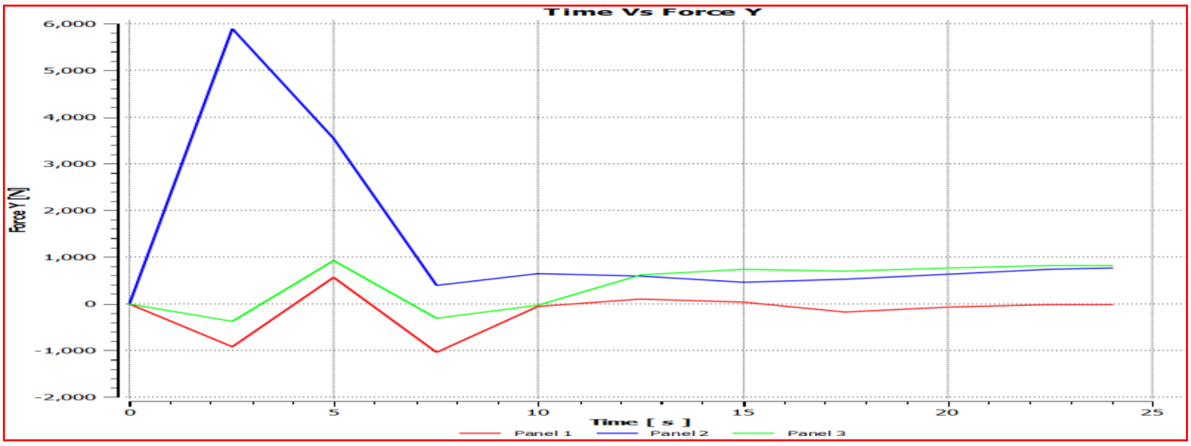

Plot.7 Time vs lift force induced on roof mounted solar panels with θ=45°, U= 25

International Journal of Technology and Applied Science (IJTAS)

E-ISSN: 2230-9004 ● Website: www.ijtas.com ● Email: editor@ijtas.com

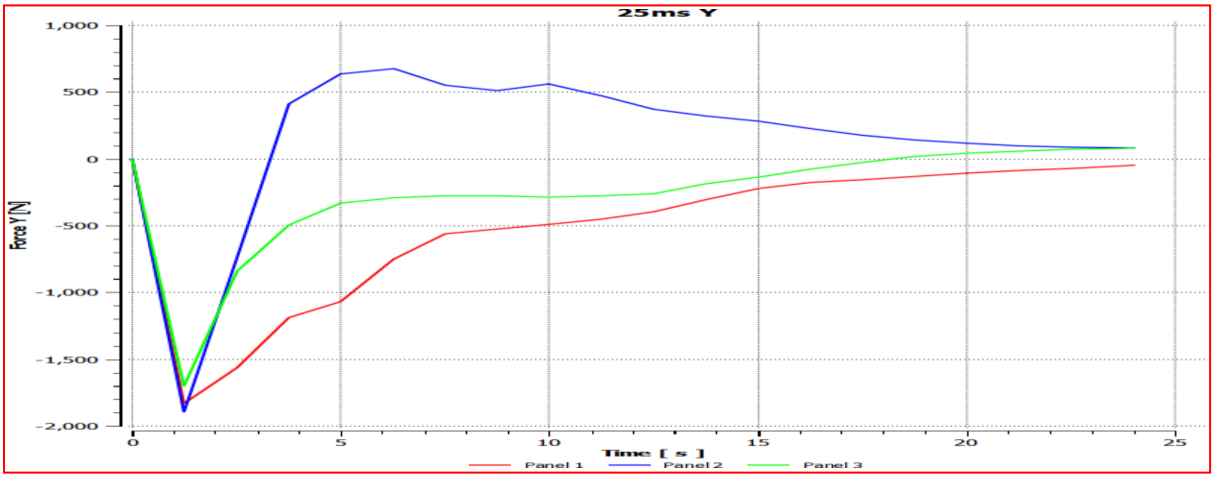

Plot.8 Time vs lift force induced on roof mounted optimized solar panels with θ= 45°, U= 25 m/s

Table .2 Lift force (Newton) comparison of roof mounted solar panels at θ=45°

Panel No	5 m/s Conventional	5 m/s Optimized	25 m/s Conventional	25 m/s Optimized
Panel1	400.16	284.19	211.943	237.637
Panel2	393.84	322.69	196.039	258.404
Panel3	339.76	311.77	248.29	229.846

When the rectangular and pentagonal panels are experiencing a wind flow with an AOA of 135° and velocities 5 m/s and 25 m/s, the lift forces induced are plotted in the format time vs lift forces induced. Plots 9 to 12 depict the above-mentioned discussion. The lift forces are induced in an unpredictable and random manner in both the conventional and optimized panels when subjected to a critical velocity. But the optimized panels tend to attain steady state at the end of time period. When the panels are exposed to normal velocity the forces induced are at a maximum of 310 N and decreases exponentially over the time in rectangular panels. But in optimized panels the maximum force induced is 100 N and tend to behave randomly throughout the time. For better understanding on how the forces are induced over the time the graphs are converted to numerical data and represented in Table 3.

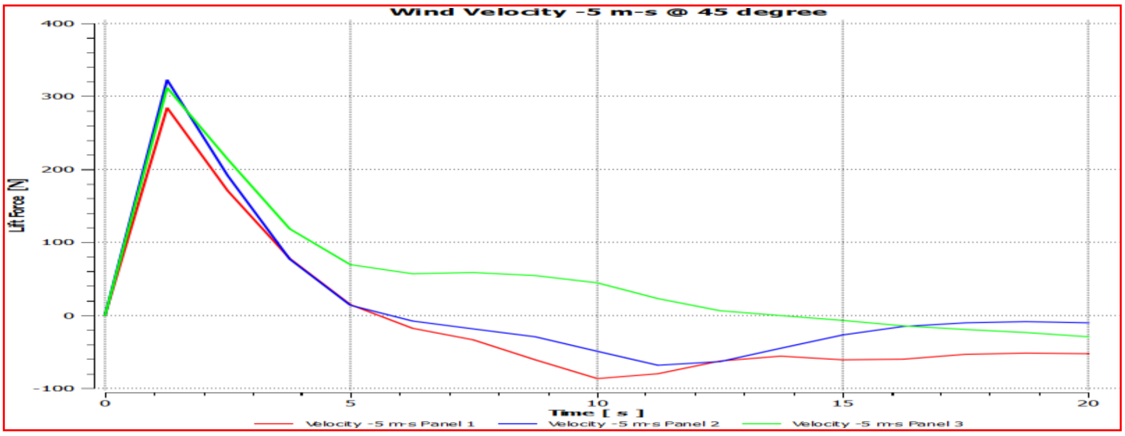

Plot.9 Time vs lift force induced on roof mounted solar panels with θ=135°,U=5 m/s

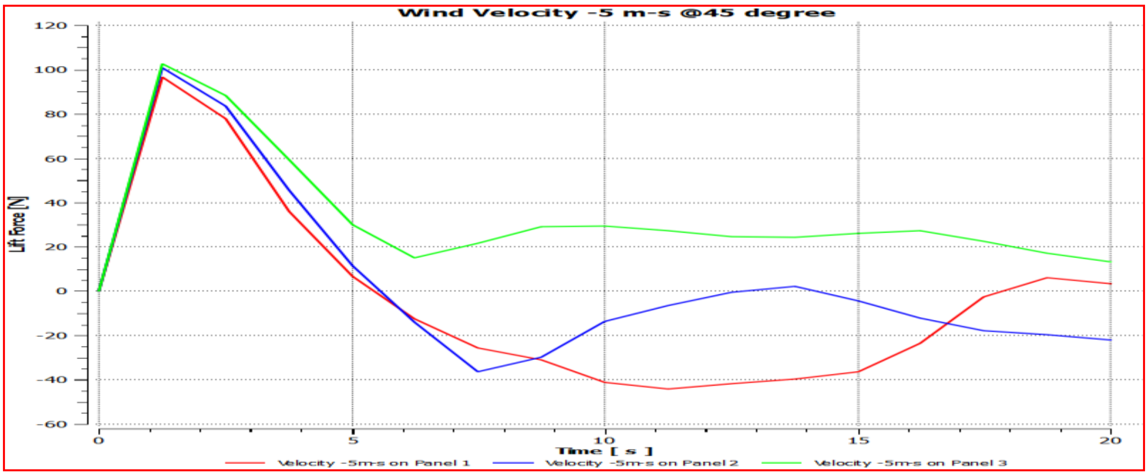

Plot.10 Time vs lift force induced on roof mounted optimized solar panels with θ= 135°, U= 5 m/s

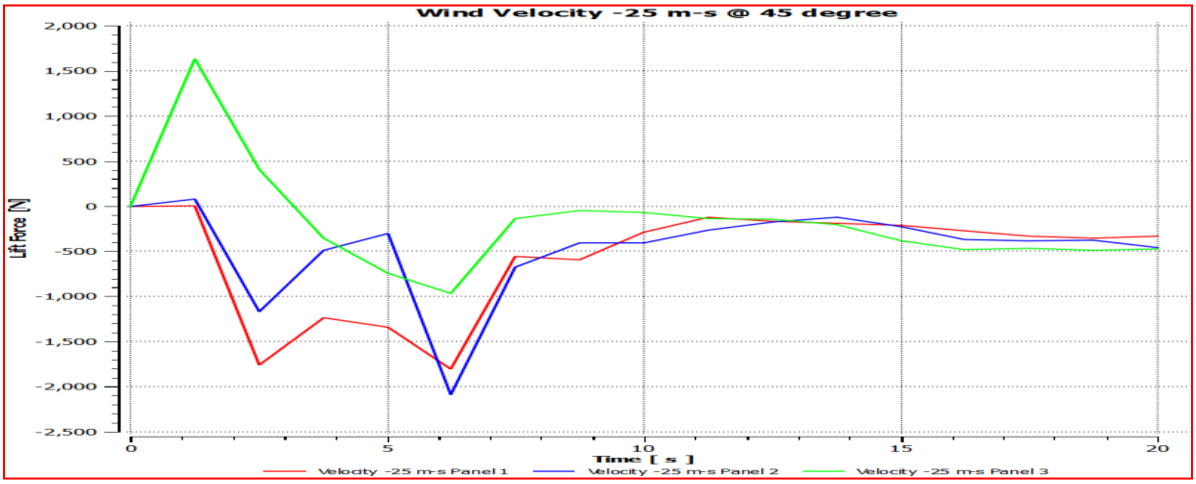

Plot.11 Timevs lift force induced on roof mounted solar panels with θ=135°,U=25m/s

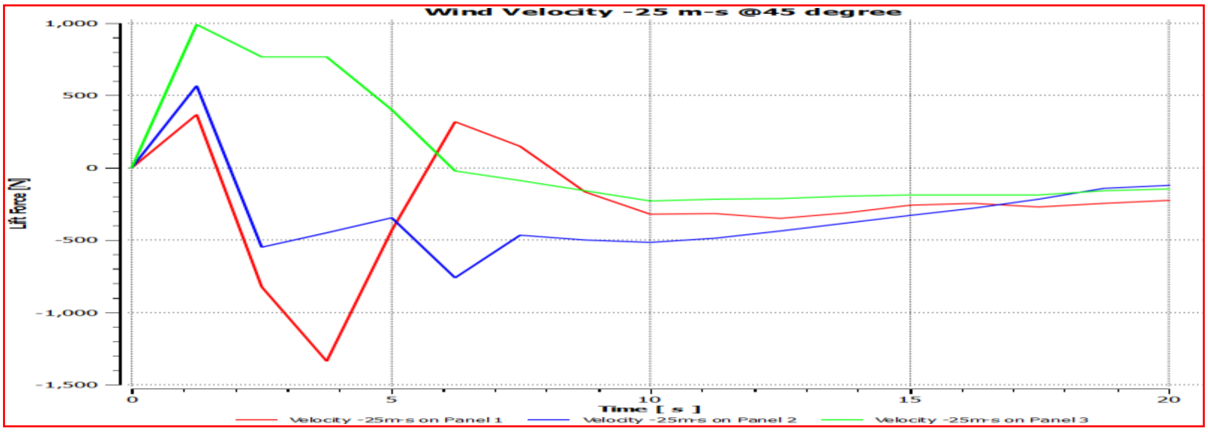

Plot.12 Time vs lift force induced on roof mounted optimized solar panels with θ= 135°, U= 25 m/s

Table .3 Lift comparison (in Newton) of roof mounted solar panels at θ=135°

Panel No	5m/s Conventional	5m/s Optimized	25m/s Conventional	25m/s Optimized
Panel1	284.19	211.943	237.637	120.65
Panel2	322.69	196.039	258.404	117.64
Panel3	311.77	248.29	229.846	111.8

Total forces acting on the roof mounted solar panels

Total forces acting the roof mounted solar panels were determined by summing up of the lift forces and drag forces. Variation of the total forces on the roof mounted solar panels for three panels for different angles of attack such as 0^0, 45^0, 130^0 and 180^0 are for the case of wind flowing at 25 m/s graphically shown in Fig.1. It is found that a maximum of 600 N is being applied on panel 1 in both the cases of 0^0 and 45^0. Fig.2 shows the effect of total wind load on solar panels for a wind speed of 5 m/s.

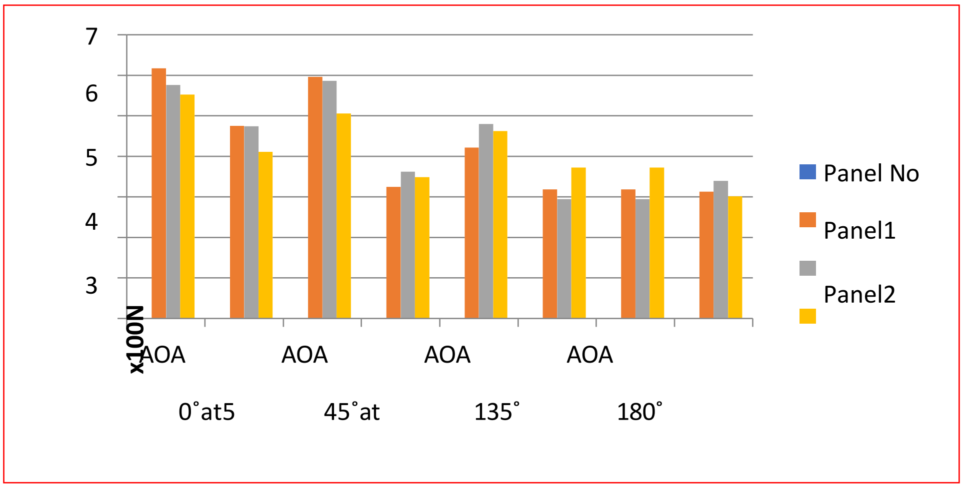

Figure 1. Total force on solar panels mounted at rooftop at 0˚, 45˚, 135˚, 180˚for 25 m/s wind Speed

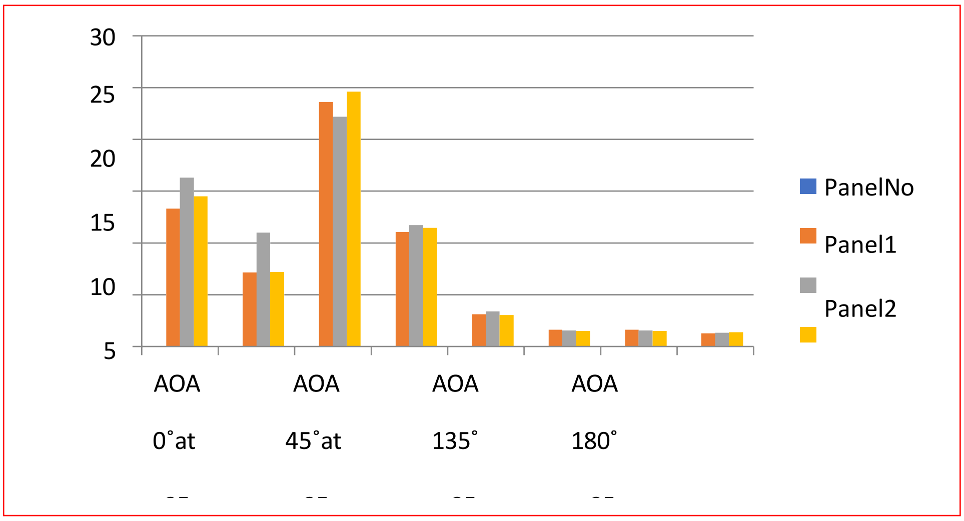

Figure 2. Total force on solar panels mounted at roof top at 0˚, 45˚, 135˚, 180˚for5 m/s

International Journal of Technology and Applied Science (IJTAS)

E-ISSN: 2230-9004 ● Website: www.ijtas.com ● Email: editor@ijtas.com

4. CONCLUSIONS

In this last test case, the panels are subjected to a wind flow with an AOA of 180^0 with velocities 5 m/s and 25 m/s. The time vs lift forces induced in these panels are plotted and represented from plot 1 to plot 12. The plots for conventional panels exposed to normal and critical velocities are illustrated in plots of odd numbered, while for optimized panels, the forces induced are represented in even numbers. When the panels are exposed to a critical velocity, i.e., 25 m/s, the maximum force induced in the conventional panels is 1000 N and in optimized panels it is 2500 N, both are in the reverse direction. As time progresses in both the panels, the forces induced are unpredictable and show no signs of convergence and steady-state.

REFERENCES:

1. P. Surendra Reddy (2019) Wind Load Analysis of Solar Farm Using Computational Fluid Dynamics International Journal of Mechanical and Production Engineering Research and Development (IJMPERD) vol. 9, No.485–498.
2. Wiser, Ryan, et al. "The environmental and public health benefits of achieving high penetrations of solar energy in the United States." *Energy*, 113 (2016): 472-486.
3. Li, Hongqiang, et al. "Exergy and environmental assessments of a novel trigeneration system taking biomass and solar energy as co-feeds." *Applied Thermal Engineering*, 104 (2016): 697-706.
4. Zeaiter, Joseph, et al. "Waste tire pyrolysis using thermal solar energy: An integrated approach." *Renewable Energy*, 123 (2018): 44-51.
5. Mehrpooya, Mehdi, and Ali Dadak. "Investigation of a combined cycle power plant coupled with a parabolic trough solar field and high-temperature energy storage system." *Energy Conversion and Management*, 171 (2018): 1662-1674.
6. Tehrani, S. Saeed Mostafavi, et al. "Annual comparative performance and cost analysis of high-temperature, sensible thermal energy storage systems integrated with a concentrated solar power plant." *Solar Energy*, 153 (2017): 153-172.
7. Hemmer, C., et al. "Early development of unsteady convective laminar flow in an inclined channel using CFD: Application to PV panels." *Solar Energy*, 146 (2017): 221-229.
8. Edgar, R., et al. "A computational fluid dynamic study of PV cell temperatures in novel platform and standard arrangements." *Solar Energy*, 144 (2017): 203-214.
9. Al-Waeli A. H. A., et al. Modelling and experimental validation of a PVT system using nanofluid coolant and nano-PCM. Solar Energy, Vol. 177, Issue 1, 2019, p. 178-191.
10. Hemmer C., et al. Early development of unsteady convective laminar flow in an inclined channel using CFD: Application to PV panels. Solar Energy, Vol. 146, 2017, p. 221-229.
11. Edgar R., et al. A computational fluid dynamic study of PV cell temperatures in novel platform and standard arrangements. Solar Energy, Vol. 144, Issue 1, 2017, p. 203-214.